Journal of Sensor Science and Technology
Vol. 29, No. 6 (2020) pp. 374-381
http://dx.doi.org/10.46670/JSST.2020.29.6.374
pISSN 1225-5475/eISSN 2093-7563

Effects of Metal–Organic Framework Membrane on Hydrogen Selectivity

Jun Min Suh[1,*], Sung Hwan Cho[1,*], and Ho Won Jang[1,+]

Abstract

Hydrogen gas has attracted considerable attention as a promising candidate for future energy resources because of its eco-friendly characteristics; however, its highly combustible characteristics should be thoroughly examined to preclude potential disasters. In this regard, a highly sensitive method for the selective detection of H_2 is extremely important. To achieve excellent H_2 selectivity, the utilization of a metal–organic framework (MOF) membrane can physically screen interfering gas molecules by restricting the size of kinetic diameters that can penetrate its nanopores. This paper summarizes the various endeavors of researchers to utilize the MOF molecular sieving layer for the development of highly selective H_2 sensors. Further, the review affords useful insights into the development of highly reliable H_2 sensors.

Keywords : Gas sensor, Hydrogen sensor, Metal–organic frameworks, Nanoporous, Membrane

1. INTRODUCTION

Hydrogen gas (H_2) has been regarded as one of the most attractive future energy resources because of its highly eco-friendly consumption mechanisms for energy generation [1]. Moreover, H_2 is well-known for its highly combustible characteristics, including low ignition energy, wide flammability range, and high combustion velocity [2]. Hence, to ensure the safe utilization of H_2, the use of highly sensitive and selective H_2-sensing technologies is advantageous. Related research investigations that have been conducted over the recent decades have found that the most effective strategies for H_2 detection include the utilization of Pd [3-6]. Palladium is well-known for forming palladium hydride (i.e., PdH_x) after exposure to H_2, resulting in resistance change (low concentration, <1%) or volume expansion (high concentration, >2%). These PdHx characteristics can be exploited for the development of highly selective H_2 sensors [7]. However, in actual applications, Pd-based H_2 sensors are exposed to ambient air containing O_2, which can reduce the efficiency of H_2-sensing by blocking the active sites of Pd lattices [8]. Accordingly, various strategies to inhibit the degradation of Pd by O_2 have been investigated. [9]

The utilization of a metal–organic framework (MOF) has been regarded as one of the most effective methodologies in this aspect; it can provide a highly selective membrane because of its easily controllable pore sizes. The MOF, which is composed of metal nodes and organic linkers, have been adopted in gas sensor applications i) as the main gas-sensing channel [10-13], ii) as a protective and selective membrane [14-18], or iii) as a pre-step material for MOF-derived gas-sensing materials [19-22]. However, the MOF itself is limited by its low conductivity and poor chemical stability with no distinct mechanism for selective H_2-sensing [23]. Moreover, the MOF-derived materials are usually metal oxides that are advantageous for detecting volatile organic compounds but without a distinct mechanism for selective H_2-sensing [24-27]. However, the MOF can provide a molecular sieving layer on top of gas-sensing materials with precisely controllable pore sizes. The MOF can be utilized for the physical screening of target gas molecules according to their kinetic diameter; this can be beneficial for achieving H_2 selectivity.

This paper summarizes the endeavors of researchers to utilize MOF as a molecular sieving layer for the development of a highly selective Pd-based H_2 sensor. These endeavors demonstrate that the use of MOF-based protective and molecular sieving layers can be a highly effective strategy for enhancing the H_2-sensing performance and lifetime of sensors. This review is anticipated to

[1] Department of Materials Science and Engineering, Research Institute of Advanced Materials, Seoul National University
Gwanak-ro 1, Gwanak-gu, Seoul 08826, Republic of Korea
[*] These authors contributed equally.
[+] Corresponding author: hwjang@snu.ac.kr
(Received: Nov. 25, 2020, Revised: Nov. 28, 2020, Accepted: Nov. 29, 2020)

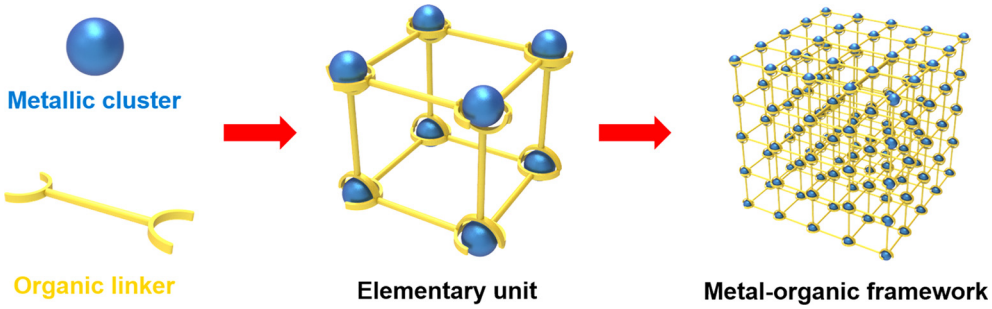

Fig. 1. Schematic of metal–organic framework

provide effective and useful insight into the development of highly reliable and potential H_2 sensors.

2. UTILIZATION OF METAL–ORGANIC FRAMEWORK MEMBRANE

2.1 Pore Size Effects of MOF Membrane

The MOF is comprised of metal nodes and organic linkers, as shown in Fig. 1, and has extremely large surface areas, highly porous structures, and various morphologies [28]. In particular, the appropriate choice of metal species and organic linkers can result in the formation of nanopores with preferred diameters that may be used for various MOF separation membranes [29]. In this regard, the MOF membrane with a pore size larger than the kinetic diameter of H_2 but smaller than those of other interfering gas molecules can lead to a highly selective detection of H_2.

M. Drobek *et al*. fabricated gas sensors based on pristine ZnO nanowires (NW) and ZnO NWs encapsulated by a thin zeolite

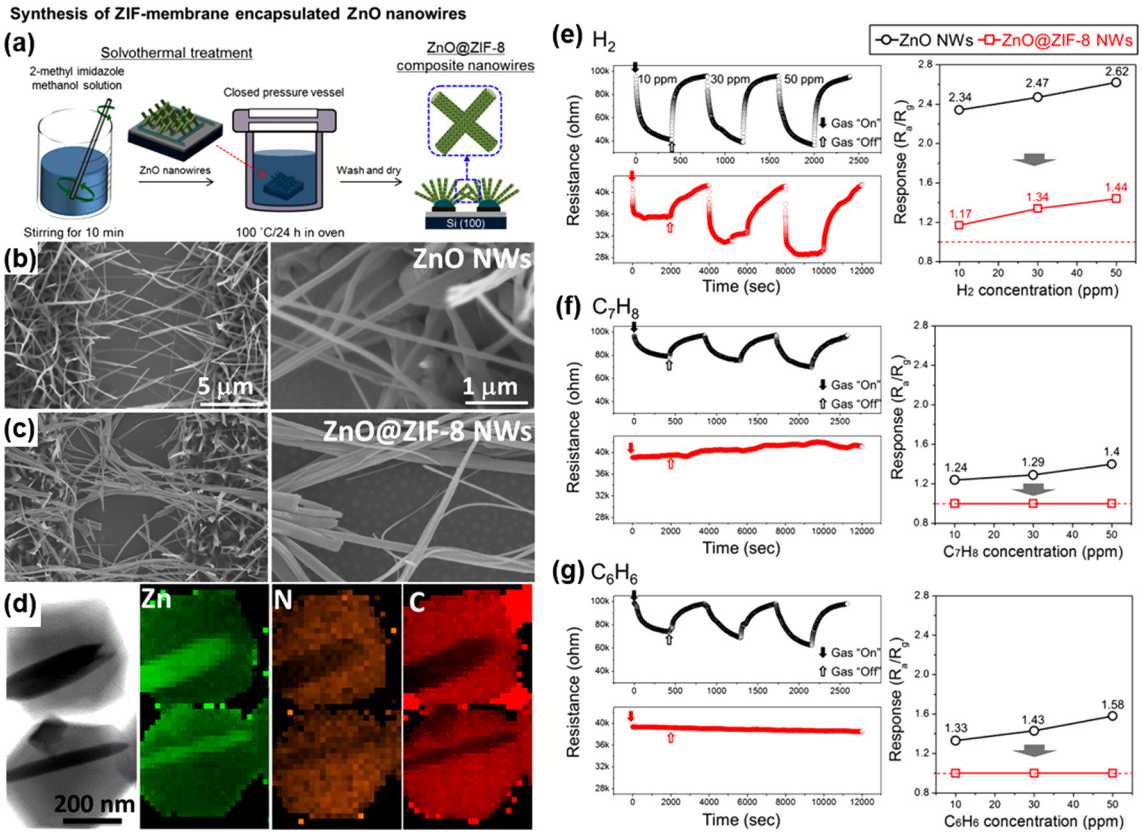

Fig. 2. (a) Schematic of the synthesis steps yielding the ZIF-membrane encapsulated ZnO nanowires (ZnO@ZIF-8 NWs). (b) Plane-view FESEM image of networked ZnO nanowires, (c) ZnO@ZIF-8 composite nanowires, and (d) TEM images of ZnO@ZIF-8 composite nanowires and the corresponding STEM/EDX cartography for Zn, N, and C elements. (e-g) Responses of the pristine ZnO nanowires and ZnO@ZIF-8 composite nanowires in contact with 10, 30, and 50 ppm single gas concentration: (e) H_2, (f) C_7H_8, and (g) C_6H_6. Reprinted with permission from [14]. Copyright © 2016 American Chemical Society.

imidazolate framework (ZIF)-8 molecular sieve membrane [14]; Fig. 2(a) shows the preparation method for the ZIF membrane-encapsulated ZnO NWs. Using the solvothermal method, the concentration of organic linkers in the reaction solution was precisely controlled for the optimized conversion of ZnO into ZIF-8. Fig. 2(b) and (c) show the scanning electron microscopy (SEM) images of the resultant ZIF membrane-encapsulated ZnO NWs. These images show the more closely stacked ZnO NWs after the solvothermal treatment for ZIF-8 encapsulation. The transmission electron microscopy (TEM) images (Fig. 2(d)) clearly show the ZIF layer encapsulating the ZnO NWs. After the optimization of fabrication procedures, the pristine ZnO NWs and ZIF-encapsulated ZnO NWs were exposed to three different target gases, including H_2, C_7H_8, and C_6H_6. As shown in Fig. 2(e)–(g), the gas responses to all three target gases decreased after the ZIF encapsulation, which certainly reduced the accessibility of target gas molecules to the ZnO NWs. The response to the 50 ppm H_2 remained at 1.44, whereas the responses to the 50 ppm C_7H_8 and C_6H_8 were practically reduced to negligibility. The prepared ZIF-8 encapsulation layer has a small portal cavity size (3.4 Å), and the kinetic diameters of C_7H_8 and C_6H_6 are 5.92 and 5.27 Å, respectively. Therefore, both C_7H_8 and C_6H_6 could not penetrate the ZIF-8 encapsulation layer; accordingly, they could not affect the surface of ZnO NWs. Meanwhile, H_2, which has a kinetic diameter of

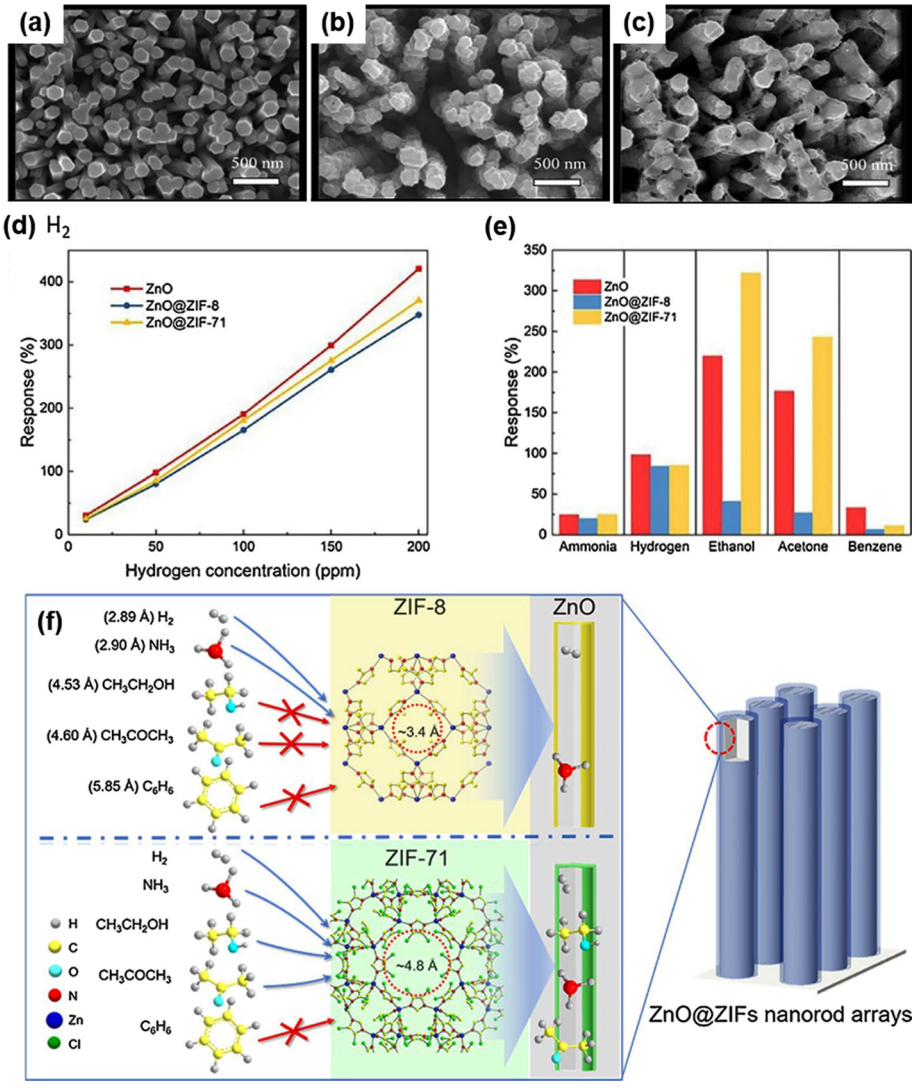

Fig. 3. (a-c) SEM images of ZnO NRAs, ZnO@ZIF-8 NRAs, ZnO@ZIF-71 NRAs: (a) for vertically-aligned ZnO NRAs, (b) for ZnO NRAs coated with ZIF-8. (c) for ZnO NRAs coated with ZIF-71. (d) Gas concentration gradient response curves of the ZnO NRAs, ZnO@ZIF-8 NRAs and ZnO@ZIF-71NRAs: these three kinds of gas sensors are exposed in hydrogen, (10, 50, 100, 150, 200 ppm) at working temperature of 250°C. (e) Gas sensing response of ZnO NRAs, ZnO@ZIF-8 NRAs and ZnO@ZIF-71 NRAs sensors to 50 ppm of different gases at 250°C. (f) The mechanism of using the difference between the pore sizes of ZIF-8 and ZIF-71 and the gas molecular sizes to select gases passing the ZIFs membrane of ZnO@ZIF NRAs. Reprinted with permission from [15]. Copyright © 2018 Elsevier B.V.

2.89 Å, could easily penetrate the ZIF-8 encapsulation layer and reach the ZnO NWs, resulting in the highly selective detection of H_2. This work demonstrates that the precise control of the MOF pore size can lead to the achievement of the desired gas selectivity depending on the kinetic diameter of the target gas molecules.

T. Zhou *et al*. investigated the effect of MOF pore sizes on gas selectivity by preparing two different MOF membranes (ZIF-8 and ZIF-71) on a ZnO nanorod array [15]. The SEM images of the hydrothermally prepared ZnO nanorods, ZnO encapsulated with ZIF-8, and ZnO encapsulated with ZIF-71 are shown in Fig. 3(a)–(c), respectively. Compared with pristine ZnO nanorods, the densely coated MOF membranes are clearly identifiable. The prepared samples were then exposed to five different target gases: NH_3, H_2, C_2H_5OH, CH_3COCH_3, and C_6H_6. Fig. 3(d) shows the gas response to H_2 as a function of H_2 concentration, and Fig. 3(e) presents the gas responses of the prepared gas sensors to all target gases. Compared with the pristine ZnO nanorods, the ZIF-8-encapsulated ZnO nanorods exhibited practically the same gas response toward NH_3 and H_2; the gas response toward C_2H_5OH, CH_3COCH_3, and C_6H_6 significantly decreased. The ZIF-71-encapsulated ZnO nanorods only exhibited a significant decrease in gas response toward C_6H_6 and maintained its gas responses to the other four target gases. The pore sizes of ZIF-8 and ZIF-71 are 3.4 and 4.8 Å, respectively; hence, the foregoing results indicate that the pore size of the ZIF membrane can determine the gas selectivity of ZnO nanorods. The NH_3, H_2, C_2H_5OH, CH_3COCH_3, and C_6H_6 gases have kinetic diameters of 2.90, 2.89, 4.53, 4.60, and 5.85 Å, respectively. Therefore, target gases with kinetic diameters smaller than that of ZIF-8 (NH_3 and H_2) could penetrate the ZIF-8 membrane, affecting the ZnO nanorods. Those with larger kinetic diameters (C_2H_5OH, CH_3COCH_3, and C_6H_6) could penetrate the ZIF-8 membrane, yielding low gas responses. For ZIF-71, only C_6H_6 exhibits a kinetic diameter larger than the pore size of the ZIF-71 membrane; thus, it is the only target gas that exhibits a decrease in gas response (Fig. 3(f)). Therefore, the precise control of the pore sizes of the MOF membrane is a potentially effective strategy for the development of gas sensors with the preferred selectivity.

2.2 Effects of MOF Membrane on Pd-based H_2 Sensors

As the most widely adopted MOF membrane for the selective detection of H_2 owing to its suitable cavity size (3.4 Å), researchers have endeavored to utilize ZIF-8 for Pd-based gas sensors.

M. Weber *et al*. developed highly sensitive and selective H_2 sensors based on ZnO NWs decorated with Pd nanoparticles; they also fabricated an MOF nanomembrane molecular sieve (ZIF-8) [16]. Fig. 4(a) shows the schematic of the preparation of vapor-grown ZnO NWs on interdigitated electrodes (IDEs), the successive decoration of Pd nanoparticles, and the conversion of the ZnO surface into ZIF-8. The prepared gas sensors based on pristine ZnO NWs, Pd-decorated ZnO NWs, and ZIF-8-encapsulated Pd-decorated ZnO NWs were then exposed to five different target gases: H_2, C_6H_6, C_2H_5OH, C_7H_8, and CH_3COCH_3. Fig. 4(b) shows the gas responses of the prepared gas sensors toward H_2 as a function of H_2 concentration. The Pd decoration significantly enhanced the gas responses toward H_2 compared with pristine ZnO NWs. These responses decreased to a certain level (2.63 for 50 ppm H_2) after the ZIF-8 encapsulation was applied because of the decreased gas accessibility. Fig. 4(c) shows the gas responses of the prepared gas sensors toward the other four target gases depending on the gas concentration. With the Pd decoration, the gas responses toward these four target gases (C_6H_6, C_2H_5OH, C_7H_8, and CH_3COCH_3) also slightly increased due to chemical sensitization effects. After the ZIF-8 encapsulation, however, all gas responses toward these four target gases were remarkably suppressed to practically negligible levels, resulting in the highly selective detection of H_2. Fig. 4(d) shows the exact mechanisms of the gas-sensing reaction and the effect of ZIF-8 encapsulation. Upon H_2 exposure, the Pd-decorated ZnO captured H_2 through the formation of PdH_x for the enhanced gas responses. By contrast, the other target gases only relied on the surface reaction through charge exchange with the surface-adsorbed oxygen species [30]. The ZIF-8 encapsulation provided a porous membrane for the exclusive penetration of H_2 for the highly selective detection of H_2 through the PdH_x formation. Although this work demonstrated the excellent feasibility of the ZIF-8 membrane for the highly selective detection of H_2 by Pd-based H_2 sensors, the prevention of Pd degradation by O_2 could not be confirmed. The main conduction channel was ZnO, and the lift time of the H_2 sensors was dependent on the ZnO stability, whereas the role of Pd was limited to the catalytic effects.

W.-T. Koo *et al*. prepared H_2 sensors based only on Pd NWs, which are suitable for investigating the effect of MOF encapsulation on Pd stability [17]. Fig. 5(a)–(d) show the SEM images of pristine Pd NWs and ZIF-8 encapsulated Pd NWs (4 h treatment). The Pd NWs were prepared by photolithography, and ZIF-8 was synthesized by solution methods. The authors manipulated the deposition time of ZIF-8 on Pd NWs (2, 4, and 6 h) to control the ZIF-8 encapsulation layer thickness. The SEM images show that after 4 h of the ZIF-8 deposition, the Pd NWs were completely

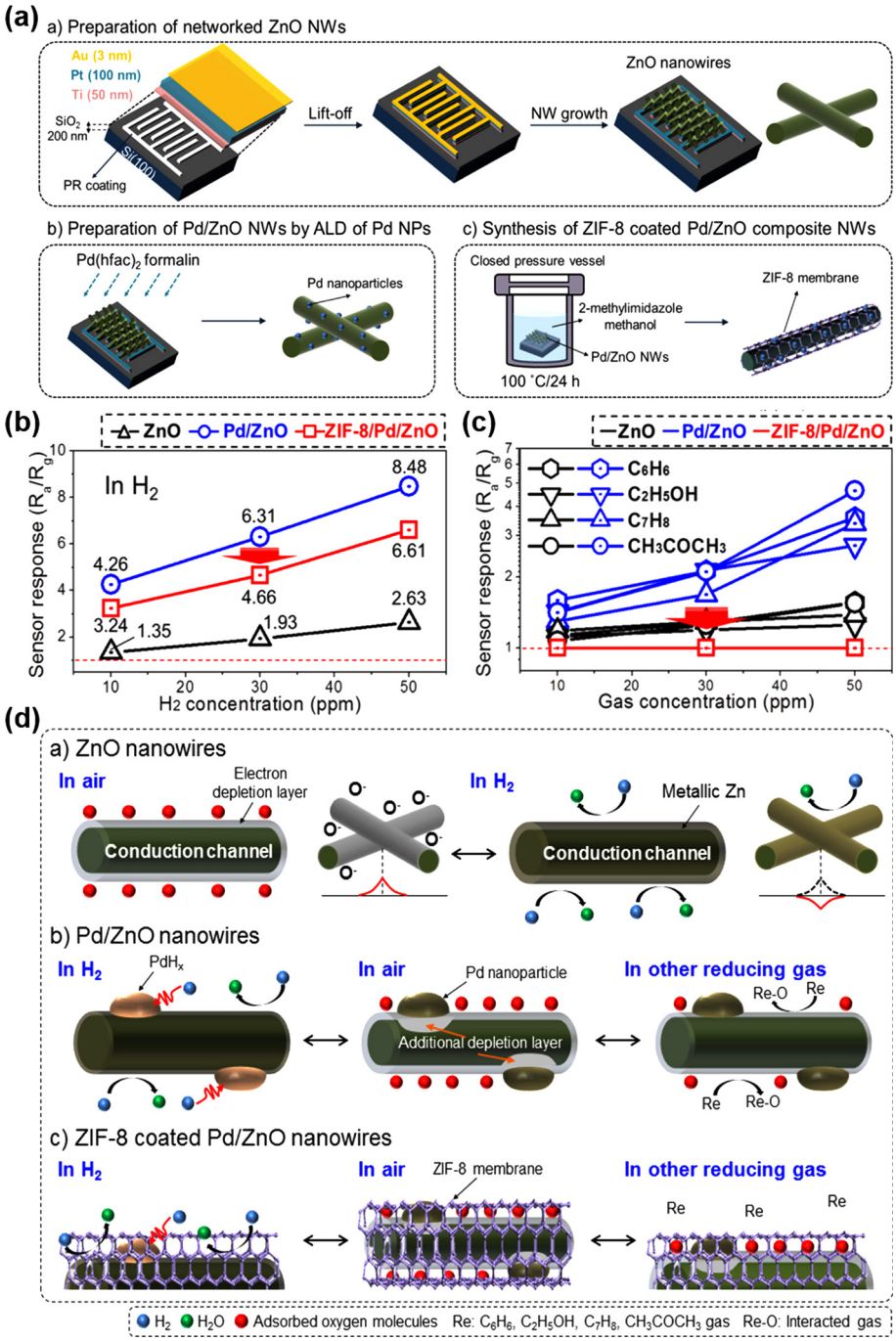

Fig. 4. (a) Schematic representation of the three key steps enabling the synthesis of the novel gas-sensing device. (b) Calibration curves of bare ZnO, Pd/ZnO, and ZIF-8/Pd/ZnO NW gas sensors to 10, 30, and 50 ppm H_2 gas. (c) Calibration curves of bare ZnO, Pd/ZnO, and ZIF-8/Pd/ZnO NW gas sensors to 10, 30, and 50 ppm H_2, C_6H_6, C_2H_5OH, C_7H_8, and CH_3COCH_3 interfering gases. (d) Schematic representation of the sensing mechanisms for a) pristine ZnO NW, b) Pd/ZnO NW and c) ZIF-8-coated Pd/ZnO NW sensors. Reprinted with permission from [16]. Copyright © 2018 American Chemical Society.

encapsulated by ZIF-8. The prepared H_2 sensors based on Pd NWs were then exposed to different concentrations of H_2 (Fig. 5(e) and (f)). The pristine Pd NWs exhibited H_2-sensing characteristics at high concentrations; however, they did not exhibit a reliable operation toward H_2 at low concentrations. Compared with pristine Pd NWs, the ZIF-8-encapsulated Pd NWs still exhibited H_2-sensing characteristics at low concentrations. The authors assumed that the unreliable H_2-sensing characteristics by the pristine Pd NWs were caused by the O_2 adsorption on the surface of Pd NWs. The reduction in the active sites on the Pd

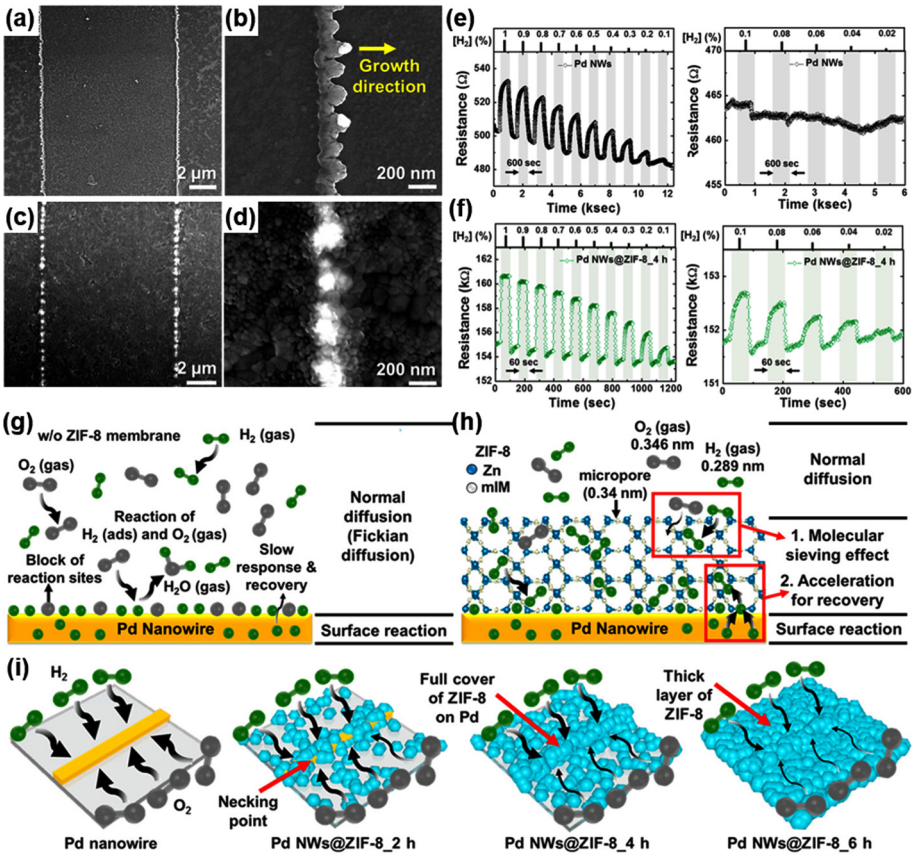

Fig. 5. SEM of Pd NWs (a, b), and Pd NWs@ZIF-8_4 h (c, d), on the glass substrate. Low-magnification SEM images of the samples with patterned Pd NWs (a gap of 10 μm) (a, c) and high-magnification SEM images of the samples (b, d). (e, f) Dynamic baseline resistance transitions in the concentration range of 0.02−1% [H_2] at RT. (e) Pd NWs, and (f) Pd NWs@ZIF-8_4 h. (g-i) Schematic illustration of accelerated hydrogen sensing properties of Pd NWs@ZIF-8. (g) Sensing model for Pd NWs without ZIF-8 membrane and (h) sensing model for Pd NWs@ZIF-8. (i) Schematic illustrate of the Pd NW, Pd NWs@ZIF-8_2 h, Pd NWs@ZIF-8_4 h, and Pd NWs@ZIF-8_6 h. Reprinted with permission from [17]. Copyright © 2017 American Chemical Society.

NWs by the O_2 adsorption limited the H_2-sensing capability of Pd NWs at low concentrations. With ZIF-8 encapsulation, however, the O_2 adsorption can be physically prevented because the kinetic diameter of O_2 (3.45 Å) is larger than the pore size of ZIF-8 (3.4 Å), resulting in the reliable H_2 sensing even at a low concentration. In addition, it was found that the response and recovery rates increased significantly after the ZIF-8 encapsulation. Different from other previously reviewed H_2 sensors, the main sensing materials are Pd NWs and not semiconducting materials, such as ZnO. Therefore, H_2 detection is mainly determined by the PdH_x formation and not the oxygen absorbate-mediated charge transfer, which is a well-known gas-sensing mechanism of metal oxide semiconductors [31]. As a result, the prevention of O_2 adsorption could lead to a highly efficient PdH_x formation and significantly improved reaction and recovery rates. Moreover, the authors attributed the acceleration effect of ZIF-8 to the adsorption and desorption rates of H_2 on Pd as a result of surface enhancement and bulk reactivity. These interpretations are well illustrated in Fig. 5(g)–(i). This work clearly demonstrated that the molecular sieving MOF membrane not only ensured the H_2 selectivity but also contributed to reliable operation and stability over a wider range of H_2 concentrations, contributing to a longer sensor lifetime.

3. CONCLUSIONS

In summary, the utilization of a nanoporous MOF membrane as a molecular sieving layer on H_2-sensing materials including metal oxide semiconductors and Pd-based materials can lead to the realization of highly selective detection of H_2. The potential H_2-sensing characteristics may be attributed to the pore-size dependent molecular sieve membrane that can selectively allow the penetration of H_2 molecules with small kinetic diameters. Moreover, the MOF membrane can prevent the O_2 adsorption on active sites on the Pd surface for reliable operation and longer

lifetime. Lastly, the effect of the MOF membrane on the acceleration of adsorption and desorption of H_2 molecules on the Pd surface are expected.

ACKNOWLEDGEMENT

This work was financially supported by National Research Foundation of Korea funded by the Ministry of Science and ICT (2016M3A7B4910, 2020M2D8A206983011) and the Strategic Core Material Development Program (No. 10080736) funded By the Ministry of Trade, Industry & Energy (MOTIE, Korea).

REFERENCES

[1] T. Hubert, L. Boon-Brett, V. Palmisano, and M. A. Bader, "Development in gas sensor technology for hydrogen safety", *Int. J. Hydrog. Energy*, Vol. 39, pp. 20474-20483, 2014.

[2] A. Gurlo and D. R. Clarke, "High-Sensitivity Hydrogen Detection: Hydrogen-Induced Swelling of Multiple Cracked Palladium Films on Compliant Substrates", *Angew. Chem. Int. Ed.*, Vol. 50, pp. 10130-10132, 2011.

[3] Y.-S. Shim, B. Jang, J. M. Suh, M. S. Noh, S. Kim, S. D. Han, Y. G. Song, D. H. Kim, C.-Y. Kang, H. W. Jang, and W. Lee, "Nanogap-controlled Pd coating for hydrogen sensitive switches and hydrogen sensors", *Sens. Actuators B*, Vol. 255, pp. 1841-1848, 2018.

[4] J. Ma, Y. Zhou, X. Bai, K. Chen, and B.-O. Guan, "High-sensitivity and fast-response fiber-tip Fabry-Perot hydrogen sensor with suspended palladium-decorated graphene", *Nanoscale*, Vol. 11, pp. 15821-15827, 2019.

[5] X. Tang, P.-A. Haddad, N. Mager, X. Geng, N. Reckinger, S. Hermans, M. Debliquy, and J.-P. Raskin, "Chemically deposited palladium nanoparticles on graphene for hydrogen sensor applications", *Sci. Rep.*, Vol. 9, pp. 3653(1)-3653(12), 2019.

[6] S. S. Kalanur, I.-H. Yoo, and H. Seo, "Pd on MoO_3 nanoplates as small-polaron-resonant eye-readable gasochromic and electrical hydrogen sensor", *Sens. Actuators B*, Vol. 247, pp. 357-365, 2017.

[7] J. M. Suh, Y.-S. Shim, K. C. Kwon, J.-M. Jeon, T. H. Lee, M. Shokouhimehr, and H. W. Jang, "Pd- and Au-Decorated MoS_2 Gas Sensors for Enhanced Selectivity", *Electron. Mater. Lett.*, Vol 14, pp. 368-376, 2019.

[8] T. B. Flanagan and W. Oates, "The Palladium-Hydrogen System", *Annu. Rev. Mater. Sci.*, Vol. 21, pp.269-304, 1991.

[9] X. Li, Y. Liu, J. C. Hemminger, and E. M. Penner, "Catalytically Activated Palladium@Platinum Nanowires for Accelerated Hydrogen Gas Detection", *ACS Nano*, Vol 9, No. 3, pp. 3215-3225, 2015.

[10] M. G. Campbell, S. F. Liu, T. M. Swager, and M. Dinca, "Chemiresistive Sensor Arrays from Conductive 2D Metal-Organic Frameworks", *J. Am. Chem. Soc.*, Vol. 137, No. 43, pp. 13780-13783, 2015.

[11] M. K. Smith and K. A. Mirica, "Self-Organized Frameworks on Textiles (SOFT): Conductive Fabrics for Simultaneous Sensing, Capture, and Filtration of Gases", *J. Am. Chem. Soc.*, Vol. 139, No. 46, 16759-16767, 2017.

[12] M. Ko, A. Aykanat, M. K. Smith, and K. A. Mirica, "Drawing Sensors with Ball-Milled Blends of Metal-Organic Frameworks and Graphite", *Sensors*, Vol. 17, No. 10, p. 2192, 2017.

[13] E.-X. Chen, H. Yang, and J. Zhang, "Zeolitic Imidazolate Framework as Formaldehyde Gas Sensor", *Inorg. Chem.*, Vol. 53, No. 11, pp. 5411-5413, 2014.

[14] M. Drobek, J.-H. Kim, M. Bechelany, C. Vallicari, A. Julbe, and S. S. Kim, "MOF-Based Membrane Encapsulated ZnO Nanowires for Enhanced Gas Sensor Selectivity", *ACS Appl. Mater. Interfaces*, Vol. 8, No. 13, pp. 8323-8328, 2016.

[15] T. Zhou, Y. Sang, X. Wang, C. Wu, D. Zeng, and C. Xie, "Pore size dependent gas-sensing selectivity based on ZnO@ZIF nanorods arrays", *Sens. Actuators B*, Vol. 258, pp. 1099-1106, 2018.

[16] M. Weber, J.-H. Kim, J.-H. Lee, J.-Y. Kim, I. Iatsunskyi, E. Coy, M. Drobek, A. Julbe, M. Bechelany, and S. S. Kim, "High-Performance Nanowire Hydrogen Sensors by Exploiting the Synergistic Effect of Pd Nanoparticles and Metal-Organic Franework Membranes", *ACS Appl. Mater. Interfaces*, Vol. 10, No. 40, pp. 34765-34773, 2018.

[17] W.-T. Koo, S. Qiao, A. F. Ogata, G. Jha, J.-S. Jang, V. T. Chen, I.-D. Kim, and R. M. Penner, "Accelerating Palladium Nanowire H_2 Sensors Using Engineered Nanofiltration", *ACS Nano*, Vol. 11, No. 9, pp. 9276-9285, 2017.

[18] P. A. Szilagyi, R. J. Westerwaal, R. Krol, H. Geerlings, and B. Dam, "Metal-organic framework thin films for protective coating of Pd-based optical hydrogen sensors", *J. Mater. Chem. C*, Vol. 1, pp. 8146-8155, 2013.

[19] P. Gao, R. Liu, H. Huang, X. Jia, and H. Pan, "MOF-templated controllable synthesis of α-Fe_2O_3 porous nanorods and their gas sensing properties", *RSC Adv.*, Vol. 6, pp. 94699(1)-94699(12), 2016.

[20] K. Rui, X. Wang, M. Du, Y. Zhang, Q. Wang, Z. Ma, Q. Zhang, D. Li, X. Huang, G. Sun, J. Zhu, and W. Huang, "Dual-Function Metal-Organic Framework-Based Wearable Fibers for Gas Probing and Energy Storage", *ACS Appl. Mater. Interfaces*, Vol. 10, No. 3, pp. 2837-2842, 2018.

[21] J.-S. Jang, W.-T. Koo, D.-H. Kim, and I.-D. Kim, "In Situ Coupling of Multidimensional MOFs for Heterogeneous Metal-Oxide Architectures: Toward Sensitive Chemiresistors", *ACS Cent. Sci.*, Vol. 4, No. 7, pp. 929-937, 2018.

[22] Y.-M. Jo, T.-H. Kim, C.-S. Lee, K. Lim, C. W. Na, F. Abdel-Hady, A. A. Wazzan, and J.-H. Lee, "Metal–Organic Framework-Derived Hollow Hierarchical Co_3O_4 Nanocages with Tunable Size and Morphology: Ultrasensitive and Highly Selective Detection of Methylbenzenes", *ACS Appl. Mater. Interfaces*, Vol. 10, No. 10, pp. 8860-8868, 2018.

[23] W.-T. Koo, J.-S. Jang, and I.-D. Kim, "Metal-Organic Frameworks for Chemiresistive Sensors", *Chem*, Vol. 5, pp. 1938-1963, 2019.

[24] Y. Lu, W. Zhan, Y. He, Y. Wang, X. Kong, Q. Kuang, Z. Xie, and L. Zheng, "MOF-Templated Synthesis of Porous Co_3O_4 Concave Nanocubes with High Specific Surface Area and Their Gas Sensing Properties", *ACS Appl. Mater. Interfaces*, Vol. 6, No. 6, pp. 4186-4195, 2014.

[25] W.-T. Koo, J.-S. Jang, S.-J. Choi, H.-J. Cho, and I.-D. Kim, "Metal–Organic Framework Templated Catalysts: Dual Sensitization of PdO–ZnO Composite on Hollow SnO_2 Nanotubes for Selective Acetone Sensors", *ACS Appl. Mater. Interfaces*, Vol. 9, No. 21, pp. 18069-18077, 2017.

[26] J.-L. Wang, Q.-G. Zhai, S.-N. Li, Y.-C. Jiang, and M.-C. Hu, "Mesoporous In_2O_3 materials prepared by solid-state thermolysis of indium-organic frameworks and their high HCHO-sensing performance", *Inorg. Chem. Commun.*, Vol. 63, pp. 48-52, 2016.

[27] W. Li, X. Wu, N. Han, J. Chen, X. Qian, Y. Deng, W. Tang, and Y. Chen, "MOF-derived hierarchical hollow ZnO nanocages with enhanced low-concentration VOCs gas-sensing performance", *Sens. Actuators B*, Vol. 225, pp. 158-166, 2016.

[28] H. Furukawa, K. E. Cordova, M. O'Keeffe, and O. M. Yaghi, "The Chemistry and Applications of Metal-Organic Frameworks", *Science*, Vol. 341, No. 6149, pp. 1230444(1)-1230444(12), 2013.

[29] S.-J. Bao, R. Krishna, Y.-B. He, J.-S. Qin, Z.-M. Su, S.-L. Li, W. Xie, D.-Y. Du, W.-W. He, S.-R. Zhang, and Y.-Q. Lan, "A stable metal-organic framework with suitable pore sizes and rich uncoordinated nitrogen atoms on the internal surface of micropores for highly efficient CO_2 capture", *J. Mater. Chem. A*, Vol. 3, pp. 7361(1)-7361(8). 2015.

[30] J. M. Suh, Y.-S. Shim, D. H. Kim, W. Sohn, Y. Jung, S. Y. Lee, S. Choi, Y. H. Kim, J.-M. Jeon, K. Hong, K. C. Kwon, S. Y. Park, C. Kim, J.-H. Lee, C.-Y. Kang, H. W. Jang, "Synergetically Selective Toluene Sensing in Hematite?Decorated Nickel Oxide Nanocorals", *Adv. Mater. Technol.* Vol. 2, p. 1600259(1)-1600259(10), 2017.

[31] J. M. Suh, W. Sohn, Y.-S. Shim, J.-S. Choi, Y. G. Song, T. L. Kim, J.-M. Jeon, K. C. Kwon, K. S. Choi, C.-Y. Kang, H.-G. Byun, H. W. Jang, "p–p Heterojunction of Nickel Oxide-Decorated Cobalt Oxide Nanorods for Enhanced Sensitivity and Selectivity toward Volatile Organic Compounds", *ACS Appl. Mater. Interfaces*, Vol. 10, pp. 1050–1058, 2017.